The organic cation transporter-3 is a pivotal modulator of neurodegeneration in the nigrostriatal dopaminergic pathway

Mei Cui[a,1], Radha Aras[a,1], Whitney V. Christian[a], Phillip M. Rappold[a], Mamata Hatwar[a], Joseph Panza[a], Vernice Jackson-Lewis[b], Jonathan A. Javitch[c], Nazzareno Ballatori[a], Serge Przedborski[b,2], and Kim Tieu[a,2]

[a]Department of Environmental Medicine, University of Rochester, Rochester, NY 14642; and [b]Departments of Neurology, Pathology, and Cell Biology and the Center for Motor Neuron Biology and Disease and [c]Center for Molecular Recognition and Departments of Psychiatry and Pharmacology, Columbia University, New York, NY 10032

Edited by Solomon H. Snyder, Johns Hopkins University School of Medicine, Baltimore, MD, and approved March 30, 2009 (received for review January 12, 2009)

Toxic organic cations can damage nigrostriatal dopaminergic pathways as seen in most parkinsonian syndromes and in some cases of illicit drug exposure. Here, we show that the organic cation transporter 3 (Oct3) is expressed in nondopaminergic cells adjacent to both the soma and terminals of midbrain dopaminergic neurons. We hypothesized that Oct3 contributes to the dopaminergic damage by bidirectionally regulating the local bioavailability of toxic species. Consistent with this view, Oct3 deletion and pharmacological inhibition hampers the release of the toxic organic cation 1-methyl-4-phenylpyridinium from astrocytes and protects against 1-methyl-4-phenyl-1,2,3,6-tetrahydropyridine-induced dopaminergic neurodegeneration in mice. Furthermore, Oct3 deletion impairs the removal of the excess extracellular dopamine induced by methamphetamine and enhances striatal dopaminergic terminal damage caused by this psychostimulant. These results may have far-reaching implications for our understanding of the mechanism of cell death in a wide range of neurodegenerative diseases and may open new avenues for neuroprotective intervention.

astrocytes | Parkinson's disease | extraneuronal monoamine transporter | dopamine | methamphetamine

Damage to the nigrostriatal dopaminergic pathways is a prominent feature in patients with parkinsonism. Studies in both the 1-methyl-4-phenyl-1,2,3,6-tetrahydropyridine (MPTP) mouse model of nigrostriatal dopaminergic degeneration and in postmortem tissues from patients with Parkinson's disease (PD) have pointed to distinct types and levels of expression of specific transporters as molecular contributors to the selective vulnerability of these neurons in pathological conditions such as PD (1). For instance, ventral midbrain dopaminergic neurons express both the plasma membrane dopamine transporter (DAT) and the vesicular monoamine transporter (VMAT-2). It has been shown that a reduction in DAT activity protects against the dopaminergic toxicity of MPTP whereas a reduction in VMAT-2 activity enhances toxicity (2). These observations have led many researchers to believe that the relative expression of these 2 transporters within a dopaminergic neuron is linked to its propensity to degenerate, for example, in PD. However, this view is limited by its focus on dopaminergic neuron transporters and by its lack of consideration for the potential noncell autonomous contribution to the degenerative process mediated by nondopaminergic cells such as astrocytes. Not only are astrocytes the most abundant cell type in the brain, but they have also been increasingly recognized for their roles in neuronal death (3–6), through their ability, for example, to regulate the extracellular levels of the toxic excitatory amino acid glutamate (7, 8). They can also convert MPTP to the active species 1-methyl-4-phenylpyridinium (MPP^+), which has been proposed to escape from the astrocytes through an unknown mechanism and accumulates into dopaminergic neurons by DAT (9).

In keeping with the potential role of transporters and of astrocytes in dopaminergic neurodegeneration, here we report that the organic cation transporter 3 (*Oct3*, *Slc22a3*), which is polyspecific to monovalent cations such as catecholamines, MPP^+ and methamphetamine (10–13), is highly expressed by astrocytes adjacent to both the soma and terminals of midbrain dopaminergic neurons. The present study demonstrates that the release of dopaminergic toxic organic cations, epitomized by MPP^+, into the extracellular space is Oct3 dependent and that both Oct3 deletion and inhibition protect against the loss of dopaminergic neurons in mice treated with the parkinsonian toxin, MPTP. However, in mice treated with methamphetamine, a psychostimulant that induces dopamine release, deletion of Oct3 increased the levels of extracellular dopamine and the loss of striatal dopaminergic fibers. Our results indicate that Oct3 may modulate dopaminergic damage by bidirectionally regulating the local bioavailability of exogenous and endogenous toxic species. These findings may thus shed light on a novel molecular scenario of neurodegeneration.

Results

Oct3 Is Expressed in Nondopaminergic Cells in the Midbrain Dopaminergic Pathways. Before determining the role of Oct3 in modulating organic cation-induced dopaminergic neurotoxicity, we sought to define Oct3 distribution in mouse brain regions known to be either sensitive [e.g., substantia nigra (SN), striatum] or resistant (e.g., cerebellum, hippocampus) to toxic organic cations such as MPP^+ and methamphetamine. Immunohistochemistry carried out with a previously validated polyclonal antibody raised against Oct3 (14) revealed varying intensities of Oct3 immunofluorescence among the brain regions of interest and distinct cellular Oct3 distribution within these selected regions (Fig. 1*A–N* and supporting information (*SI*) Table S1 and Fig. S1). For instance, at a regional level, both SN and striatum were intensely immunostained for Oct3, but, at a cellular level, no Oct3 immunoreactivity was detected in dopaminergic neuronal cell bodies and processes (Fig. 1 *A–C* and *G–I*). In contrast, within these brain regions, Oct3 immunoreactivity was detected in astrocytes and in nondopaminergic neurons (Fig. 1 *D–F* and *J–L*). We also detected robust Oct3 immunoreactivity in the cerebellum and dentate gyrus (Fig. 1 *M* and *N*), but in these regions,

Author contributions: M.C., R.A., W.V.C., P.M.R., M.H., J.A.J., N.B., S.P., and K.T. designed research; M.C., R.A., W.V.C., P.M.R., M.H., J.P., V.J.-L., and K.T. performed research; J.A.J. contributed new reagents/analytic tools; M.C., R.A., W.V.C., M.H., V.J.-L., J.A.J., N.B., S.P., and K.T. analyzed data; and S.P., and K.T. wrote the paper.

The authors declare no conflict of interest.

This article is a PNAS Direct Submission.

[1]M.C. and R.A. contributed equally to this work.

[2]To whom correspondence may be addressed. E-mail: kim_tieu@urmc.rochester.edu or sp30@columbia.edu.

This article contains supporting information online at www.pnas.org/cgi/content/full/0900358106/DCSupplemental.

NEUROSCIENCE

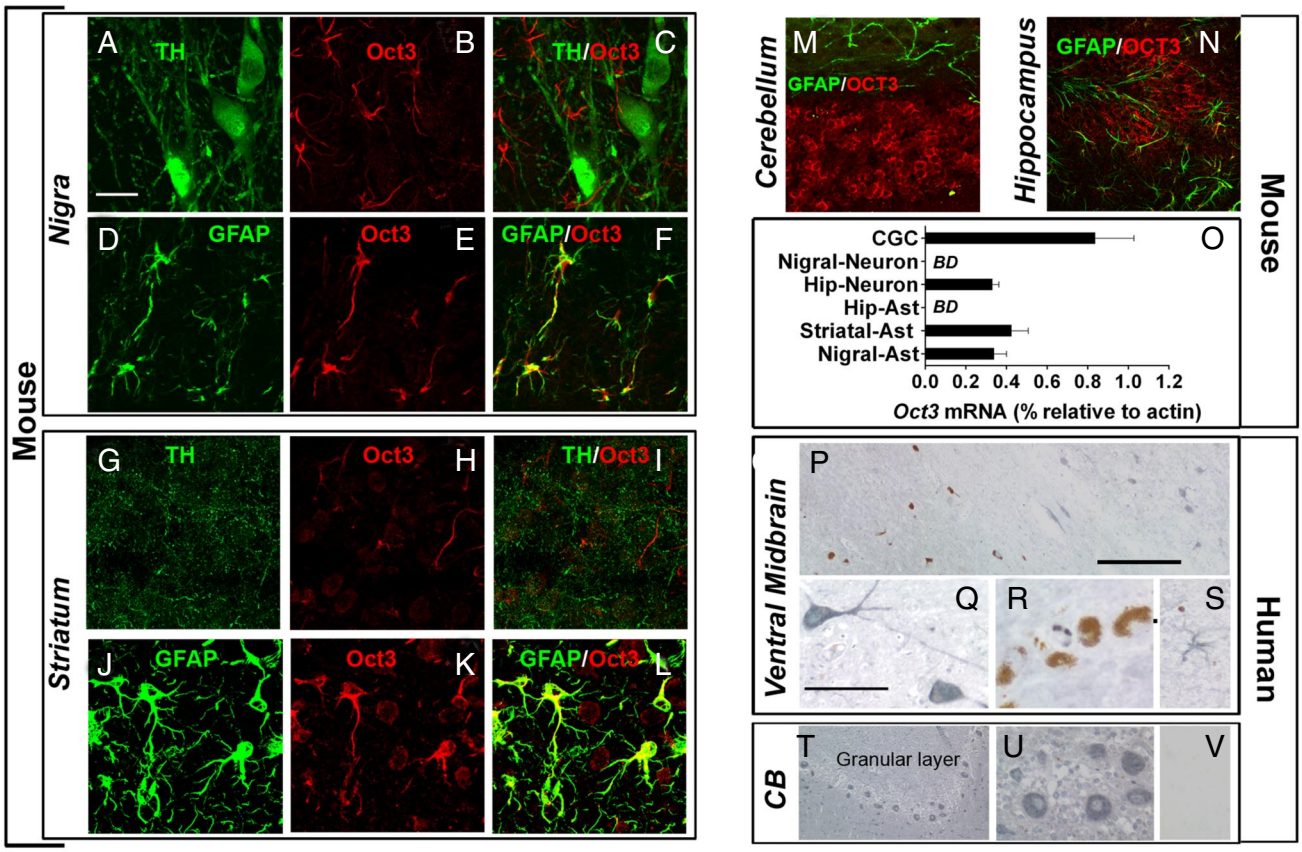

Fig. 1. Selective expression of Oct3 in the brain. Coronal mouse brain sections (*A–N*) were immunolabeled with antibodies against Oct3 in combination with either anti-TH (dopaminergic marker), anti-GFAP (astrocytic marker), or anti-MAP2 (neuronal marker). Oct3 colocalized with GFAP in the nigrostriatal region (*D–F* and *J–L*) but not with astrocytes in other regions (*M* and *N*). Although not detectable in dopaminergic structures (*A–C* and *G–I*), Oct3 immunoreactivity was detectable in other neurons (*K*, *M*, and *N*). The expression of Oct3 was further confirmed in cells captured by laser capture microdissection followed by quantitative real time RT-PCR analysis (*O*; BD, below detection). Primarily based on specific cellular markers, at least 800–1,000 cells of each type were captured. In postmortem human samples (*P–V*), OCT3 (blue–gray appearance) was robustly expressed in cells with morphology resembling that of nondopaminergic neurons (*Q*, *T*, and *U*) and astrocyte-like cells (*S*) but not in dopaminergic neurons (brown pigment of neuromelanin; *P* and *R*). As a negative control, Oct3 antibody was preabsorbed with Oct3 peptide and incubated with an adjacent cerebellar section (*V*). [Scale bars: 20 μm (*A–N*); 400 μm (*P* and *T*); and 100 μm (*Q–S*, *U*, and *V*)].

Oct3 was localized in neurons and not in astrocytes. This region-dependent neuron/astrocyte partition of Oct3 was confirmed by laser capture microdissection followed by quantitative real time RT-PCR (Fig. 1*O*). For this experiment, specific individual cells were captured on the basis of specific cellular markers (Fig. S2). To demonstrate whether the differential cellular distribution of Oct3 between the SN and the cerebellum in mice is also seen in humans, paraffin-embedded sections of ventral midbrain and cerebellum from control subjects and patients with PD (Fig. 1 *P–V*) were assessed using immunohistochemistry. Human SN dopaminergic neurons can readily be identified by their content of brown pigment, neuromelanin. Consistent with the mouse data, neuromelanin-containing neurons did not immunostain for human OCT3 (blue–gray, Fig. 1 *P* and *R*). In contrast, cells with morphology consistent with nondopaminergic neurons (Fig. 1 *P* and *Q*) and astrocytes (Fig. 1*S*) did exhibit robust immunoreactivity for this cationic transporter. OCT3 was also highly expressed in cerebellar granule neurons (Fig. 1 *T* and *U*). Thus, these results indicate that OCT3 is primarily present in nondopaminergic cells within the nigrostriatal dopaminergic pathway in both mice and humans. This argues against OCT3 regulating the entry of toxic cations into dopaminergic cells, but suggests that OCT3 may regulate their extracellular bioavailability.

Oct3 Functions Bidirectionally in Astrocytes. To determine whether Oct3 regulates extracellular concentrations of toxic organic cations, we assessed Oct3 activity in both the modified human embryonic kidney 293 cells (EM4) stably transfected with either rat Oct3 or empty vector, and in primary astrocytes. In Oct3 stably transfected EM4 cells (Fig. 2 *A–D*, see Fig. S3 regarding the generation of these cells), the transport of [^{3}H]-MPP$^+$, a stable substrate for Oct3 (13), was bidirectional, dose- and time-dependent, saturable, and inhibitable by decynium 22 (D22, an Oct3 inhibitor). In contrast, in empty vector stably transfected EM4 control cells, no transport of [^{3}H]-MPP$^+$ in either direction was detected. In the postnatal primary astrocytes, under the same experimental conditions, the transport of [^{3}H]-MPP$^+$ exhibited the same characteristics as those found in Oct3 stably transfected EM4 cells (Fig. 2 *E–G*). The important role played by Oct3 in the transport of organic cations in astrocytes is supported further by our demonstration that the uptake of [^{3}H]-MPP$^+$ is reduced by ≈3-fold in primary astrocytes cultured from *Oct3*$^{-/-}$ mice compared to that in primary astrocytes cultured from their *Oct3*$^{+/+}$ counterparts (Fig. 2 *H–J*). These results demonstrate that Oct3 expressed in primary astrocytes transport organic cations in a bidirectional manner and suggest that astrocytes may be capable of regulating both the release and the uptake of toxic species. However, these data also suggest that although Oct3 may play a dominant role, it is not the sole transporter in astrocytes regulating the bioavailability of organic cations, because some uptake of [^{3}H]-MPP$^+$ still occurred in the absence or inhibition of Oct3.

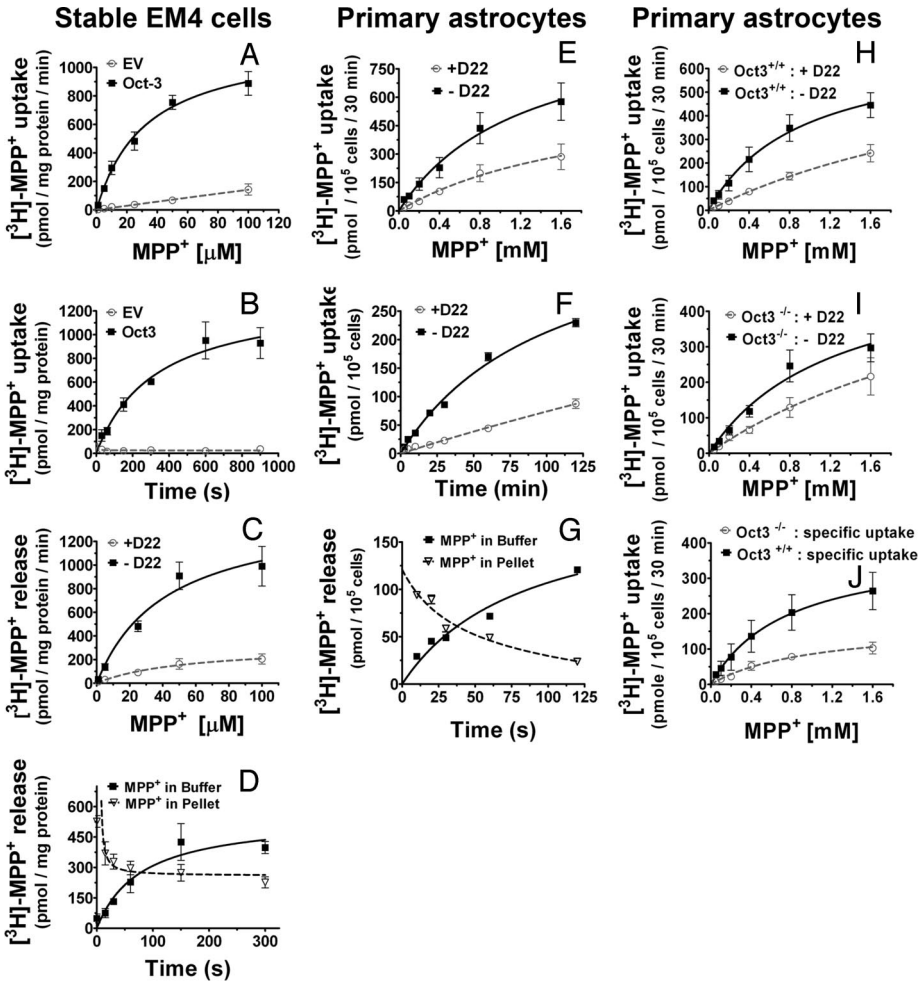

Fig. 2. Bidirectional transport of MPP^+. (*A–D*) EM4 cells stably overexpressing rat Oct3 or empty vector (EV), astrocytes from new born C57BL/6 mice (*E–G*), astrocytes from $Oct3^{+/+}$ and $Oct3^{-/-}$ mice (*H–J*), were assessed for their transport activities of $[^3H]$-MPP^+. As described in the *SI Materials and Methods*, briefly, for the uptake studies (*A*, *B*, *E*, *F*, and *H–J*), cells were incubated with 10 nM $[^3H]$-MPP^+ and various concentrations of unlabeled MPP^+, in the presence or absence of 5 μM D22 (a potent Oct3 inhibitor). Cell pellets were collected and radioactivity was counted using a scintillation counter. Specific uptake (in *J*) represents transport activity in the absence of D22 minus that of the group with D22. For the release studies (*C*, *D*, *G*), cells were preloaded for 20 min with 10 nM $[^3H]$-MPP^+ (plus 100 μM MPP^+), washed, and then incubated at 37 °C for different time points in the assay buffer with or without 5 μM D22. Radioactivity released into the buffer and remaining in cells was counted using a scintillation counter. Oct3-mediated transport was time and concentration dependent and was blocked by D22 and Oct3 deficiency. Data represent mean ± SEM from 3–5 independent experiments with $n = 4$ per experiment.

Oct3 Modulates Neurodegeneration via the Release of Toxic Cations from Astrocytes. Given the above findings, we turned to the MPTP mouse model, which is widely used to produce parkinson-like nigrostrial dopaminergic neurodegeneration (1). In astrocytes, this protoxin is converted to its active metabolite, MPP^+. This model thus affords a unique opportunity to assess the significance of the release of a toxic organic cation through Oct3 on the death of dopaminergic neurons. In saline-injected $Oct3^{+/+}$ and $Oct3^{-/-}$ mice, there was no difference in stereological counts of SN par compacta (SNpc) dopaminergic neurons (Fig. 3*A*, *C*, and *I*) or in optical density in striatal dopaminergic innervation (Fig. 3 *E*, *G*, and *J*), as evidenced by immunostaining for the rate-limiting enzyme in DA synthesis, tyrosine hydroxylase (TH). In MPTP-injected $Oct3^{+/+}$ mice, there was a loss of SNpc TH^+ neurons (Fig. 3 *B* and *I*) and of striatal TH^+ fibers (Fig. 3 *F* and *J*). In contrast, in MPTP-injected $Oct3^{-/-}$ mice, the dopaminergic cell loss was markedly attenuated (Fig. 3 *D* and *H–J*). Similar protection against MPTP was observed when Oct3 was inhibited by the administration of D22 in $Oct3^{+/+}$ mice (Fig. 3 *K* and *L*).

If most of the MPP^+ produced within astrocytes was trapped because of the absence or the inhibition of Oct3, the resulting high intra-astrocyte MPP^+ levels may kill these cells. To address this concern, we evaluated the sensitivity of astrocytes to MPP^+ by incubating these primary cells with 400 μM MPP^+ for 24 h, a regimen that induced ≈50% of loss in cell viability in the immortalized rat dopaminergic N27 neurons (Fig. S4*A*). Under these conditions, no death of astrocytes was detected (Fig. S4*B*). Similar resistance was observed when 400 μM of paraquat were used to induce oxidative stress. These data are consistent with the notion that astrocytes are inherently more resistant to toxic insults than neurons perhaps because of their high antioxidant capacity and high glycolytic rate.

The dopaminergic toxicity of MPTP correlates with the bioavailability of its active metabolite, MPP^+ (15). To assess whether D22 treatment or Oct3 ablation interferes with the conversion of MPTP into MPP^+, wild-type C57BL/6 mice infused with D22 and $Oct3^{-/-}$ mice were injected with MPTP and striatal tissue levels of MPP^+ were measured. There was no difference in MPP^+ levels between mice that received D22 or vehicle (Fig. S5*A*) nor between $Oct3^{-/-}$ and $Oct3^{+/+}$ mice (Fig. S5*B*). MPP^+-induced dopaminergic neurotoxicity also depends on its uptake into dopaminergic neurons via DAT (9). There was no alteration in DAT protein content in the $Oct3^{-/-}$ animals as compared to their wild-type littermates (Fig. S5*C*). We also assessed the potency of D22 to antagonize MPP^+ transport by DAT in EM4 cells overexpressing mouse DAT. D22 inhibited transport by DAT with an IC_{50} of 45.0 ± 4.2 μM ($n = 5$), whereas the IC_{50} values of D22 for Oct3 are in the low nanomolar range (16) making D22 more than 1,000-fold less potent at DAT than at Oct3. Thus, the above genetic and pharmacological data indicate that Oct3 plays a critical role in modulating the demise of dopaminergic neurons and suggest that this protective effect stems from Oct3 regulation of the outflow of MPP^+ from the neighboring astrocytes. This observation is consistent with the previous suggestion that MPP^+ is released from astrocytes (9).

Oct3 Affects Striatal Levels of MPP^+ and Dopamine. To support further that Oct3 regulates the release of toxic organic cations under in vivo settings, microdialysis in freely moving mice was

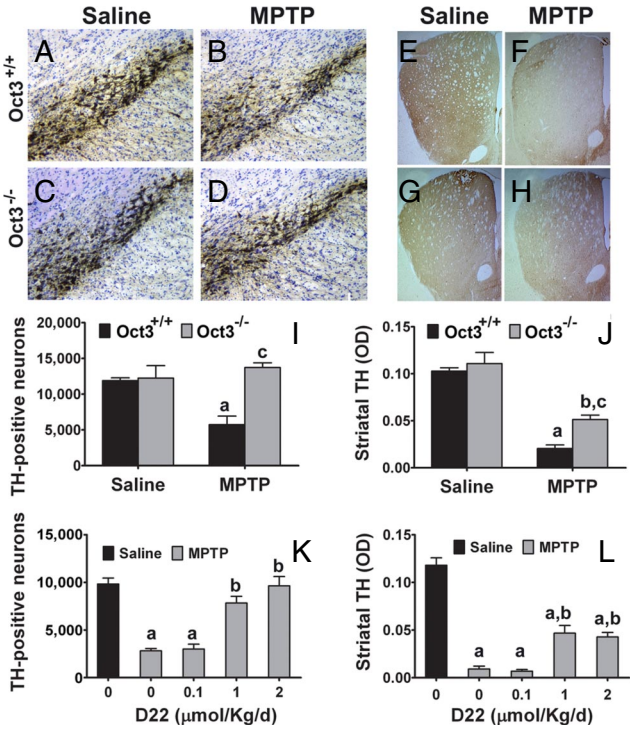

Fig. 3. Inhibition/ablation of Oct3 protected against MPTP neurotoxicity. *Oct3*$^{-/-}$ mice and their wild-type littermates *Oct3*$^{+/+}$ (*A–J*), and C57BL/6 mice (*K* and *L*) infused s.c. with either saline or varying doses of D22, were injected with MPTP or saline. The loss of TH-positive neurons in the nigra (*A–D* and *I*) was completely prevented in the *Oct3*$^{-/-}$ mice (*I*) and by D22 (*K*, in a dose-dependent manner). Damage to the striatal density of TH-positive fibers (*E–H*, *J*, and *L*) was also attenuated in these animals. (*I* and *J*) (*a*) $P < 0.01$ compared to the *Oct3*$^{+/+}$ saline group; (*b*) $P < 0.01$ compared to the *Oct3*$^{-/-}$ saline group; (*c*) $P < 0.05$ compared to the *Oct3*$^{+/+}$ MPTP group, analyzed by 2-way ANOVA with treatments crossed with genotypes (panel *I*: genotype: $F_{1,15} = 8.70$, $P = 0.01$; treatment: $F_{1,15} = 2.99$, $P = 0.10$; panel *J* genotype: $F_{1,15}$: $= 6.60$, $P = 0.021$; treatment: $F_{1,15} = 67.07$, $P < 0.001$) followed by the Newman-Keuls *posthoc* test. (*K* and *L*) (*a*) $P < 0.01$ compared to the control saline group; (*b*) $P < 0.05$ compared to the MPTP group without D22, analyzed by 1-way ANOVA followed by the Newman-Keuls post hoc test (panel *K*: $F_{4,13} = 30.13$, $P < 0.001$; panel *L*: $F_{4,14} = 55.37$, $P < 0.001$). Data represent mean ± SEM from 3–5 animals per group.

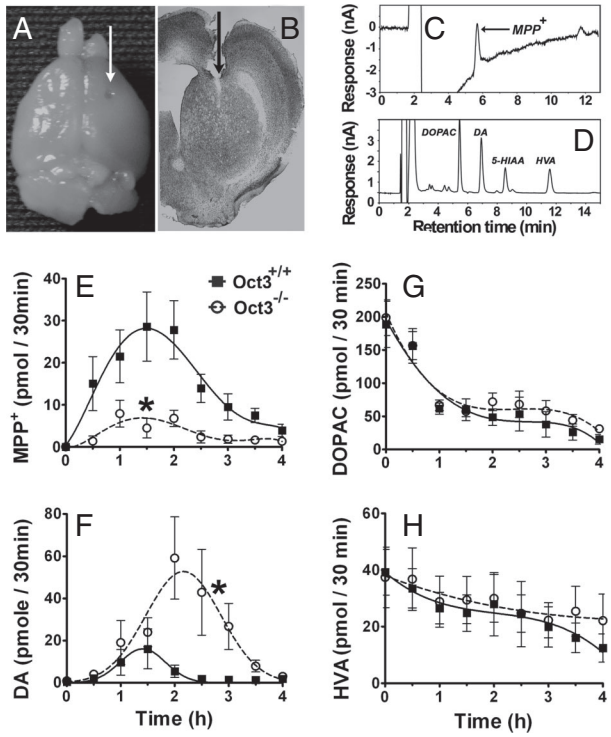

Fig. 4. Oct3 ablation altered extracellular levels of MPP$^+$ and DA in MPTP injected mice. *Oct3*$^{-/-}$ and their *Oct3*$^{+/+}$ littermates were stereotaxically implanted with microdialysis probes into the right striatum (*A*), as verified in coronal striatal sections stained with thionin (*B*). Dialysates were collected every 30 min for 1 h before MPTP injection (30 mg/kg, i.p.) for baseline measurements (pooled for 0 time point) and for an additional 4 h after the injection, followed by HPLC analyses for the levels of MPP$^+$ (*E*), DA (*F*), and its metabolites (*G* and *H*). Representative HPLC chromatograms for these measurements at 90 min after MPTP injection were illustrated in *C* and *D*. Data represent mean ± SEM, $n = 9$ WT and 11 KO. Areas under the curve were generated using GraphPad Prism followed by a 2-tailed *t* test. ⋆, $P < 0.05$ compared to the *Oct3*$^{+/+}$ group.

performed. From the microdialysis probes implanted into the striatum (Fig. 4*A* and *B*), fractions of brain dialysates were collected every 30 min for 1 h before (to determine the baseline levels) and 4 h after MPTP injection. Thirty minutes after the injection of MPTP, extracellular MPP$^+$ became detectable in the *Oct3*$^{+/+}$ mice and rose thereafter (Fig. 4*E*). In *Oct3*$^{-/-}$ mice, extracellular MPP$^+$ levels were ≈4-fold lower than those in the *Oct3*$^{+/+}$mice (Fig. 4*E*). These significantly lower levels of extracellular MPP$^+$ available to dopaminergic cells are consistent with the above mechanistic hypothesis and with the lack of cell death (Fig. 3). However, in *Oct3*$^{-/-}$ mice, the microdialysis levels of MPP$^+$ were not null, suggesting that some extracellular MPP$^+$ may be released from either astrocytes (via an Oct3-independent release) or serotonergic terminals, in which MPTP can also be metabolized to MPP$^+$.

From these same animals, changes in the levels of DA and its metabolites [3,4-dihydroxy-phenylacetic acid (DOPAC) and homovanillic acid (HVA), Fig. 4 *F–H*] were measured. It has been established that MPP$^+$ enters vesicles and induces an efflux of dopamine into the cytosol and extracellular space (17–20). Coincident with the appearance of MPP$^+$ in the extracellular compartment, there was an increase in striatal DA release with a peak at the 60- to 90-min interval in the *Oct3*$^{+/+}$ mice. In *Oct3*$^{-/-}$ mice, the DA levels were ≈5-fold higher compared to those in *Oct3*$^{+/+}$ mice (Fig. 4*F*); we noted that in these mice the peak was not only higher but also delayed (Fig. 4*F*). Although these results appear unexpected because of the lower MPP$^+$ levels in the *Oct3*$^{-/-}$ mice, they are consistent with the fact that a low amount of MPP$^+$ is sufficient to induce DA efflux (19, 20) and consistent with the role of Oct3 in removing excess extracellular DA. That is, in these mutant mice, in the absence of Oct3, the efflux of DA induced by MPP$^+$ would lead to a higher DA level in the extracellular space because of reduced clearance. Because DA can readily be oxidized, it is possible that the incomplete protection of the striatal dopaminergic terminals seen in the *Oct3*$^{-/-}$ mice (Fig. 3) was a result of damage induced by DA-related reactive species.

Oct3 Modulates Neurodegeneration via the Uptake of Extracellular Toxic Molecules. Methamphetamine induces massive efflux of DA from dopaminergic neurons, and both methamphetamine and DA are substrates of Oct3 (11, 13). Methamphetamine thus affords the opportunity to assess the function of Oct3 in the clearance of neurotransmitters and to support further the hypothesis that excess extracellular DA, in the context of deficient Oct3 function, causes striatal dopaminergic fiber damage. To examine neurotransmitter levels, an in vivo microdialysis study was performed using 2 doses of methamphetamine. At a low dose (5 mg/kg i.p.), although efflux of DA was induced, no significant difference between genotypes was detectable (Fig. 5*A*). Because DAT is a high-affinity and low-capacity transporter, whereas Oct3 is a low-affinity and high-capacity transporter, Oct3 would not be involved in the clearance of extracellular DA unless DAT is saturated by a high level of DA.

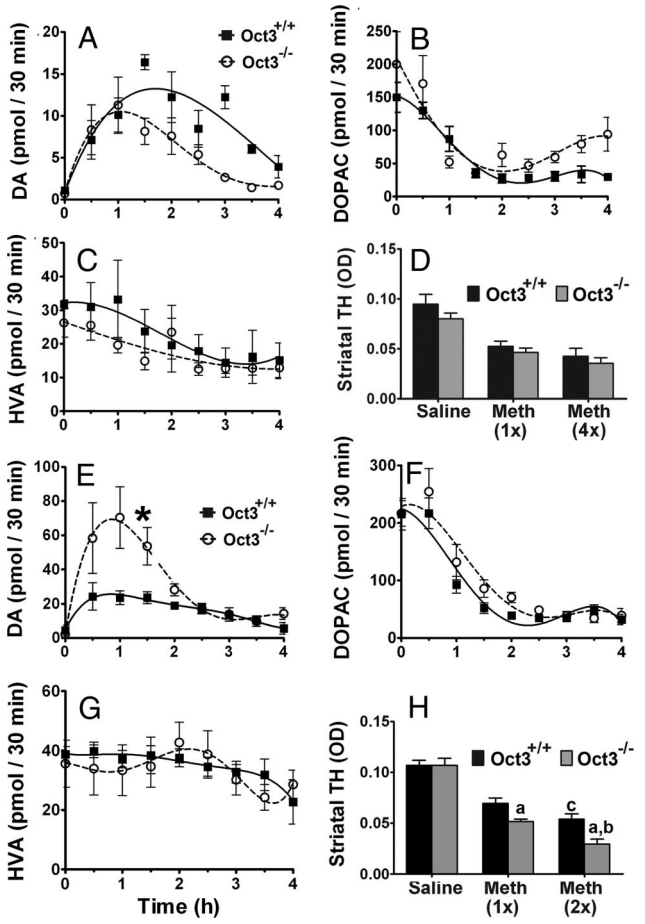

Fig. 5. Oct3 ablation increased extracellular levels of DA and striatal neurotoxicity in methamphetamine injected mice. Striatal microdialysis dialysates were collected every 30 min for 1 h before methamphetamine injections (*A–C*: 5 mg/kg i.p., *E–G*: 30 mg/kg s.c.) for baseline measurements (pooled for 0 time point) and for an additional 4 h after the injection, followed by HPLC analyses for DA (*A* and *E*) and its metabolite levels (*B*, *C*, *F*, and *G*). Data represent mean ± SEM, $n = 4–5$ per genotype. Areas under the curve were generated using GraphPad Prism followed by a 2-tailed *t* test. *, $P < 0.05$ compared to the $Oct3^{+/+}$ group. In other separate studies, animals were injected with either 5 mg/kg i.p. (single or every 2 h for 4 injections, *D*) or 30 mg/kg s.c. (single or 2 injections 4 h apart, *H*) and processed for striatal dopaminergic terminal density (*D* and *H*). Data represent mean ± SEM, $n = 3–5$ per group (*D*), $n = 6–9$ per group (*H*), (*a*) $P < 0.05$ compared to the respective $Oct3^{+/+}$ methamphetamine group, (*b*) $P < 0.01$ compared to the $Oct3^{-/-}$ methamphetamine 1 injection group, (*c*) $P < 0.05$ compared to the $Oct3^{+/+}$ methamphetamine 1 injection group, analyzed by 2-way ANOVA with treatments crossed with genotypes (genotype: $F_{1,38} = 11.19$, $P = 0.002$; treatment: $F_{2,38} = 78.86$, $P < 0.001$) followed by the Newman-Keuls post hoc test.

Consistent with this view is our observation that, after a higher dose of methamphetamine (30 mg/kg s.c.), levels of DA are more than twice as high in $Oct3^{-/-}$ than in $Oct3^{+/+}$ mice (Fig. 5*E*).

Next, mice were injected with different doses of methamphetamine and the density of striatal dopaminergic terminals, which are highly sensitive to methamphetamine toxicity, was examined. At a dose of 5 mg/kg where there was no difference in the extracellular level of DA between $Oct3^{+/+}$ and $Oct3^{-/-}$ mice, no difference in neurotoxicity was detected using either 1 injection or 4 injections every 2 h apart (Fig. 5*D*). However, at a dose (30 mg/kg s.c.) that produced higher DA levels in $Oct3^{-/-}$ mice, significantly greater loss of striatal nerve terminals was detected in these knockout mice (Fig. 5*H*). These results were confirmed by additional immunohistochemical studies aimed at labeling DAT as a second phenotypic marker of dopaminergic terminals.

Discussion

The present study demonstrates that while Oct3 is ubiquitously expressed in the brain (14, 21, 22), its cellular partition between astrocytes and neurons and among neuronal subpopulations is region specific. In particular, Oct3 immunoreactivity was detected in the nigrostriatal astrocytes, but not in astrocytes from regions such as cerebellum, hippocampus, and cortex. Also notable is the lack of Oct3 immunoreactivity in dopaminergic structures from ventral midbrain and striatum. The veracity of this striking Oct3 immunohistochemical cellular dichotomy was confirmed by quantitative real time RT-PCR analyses of samples obtained from laser capture microdissection. Furthermore, our study shows that Oct3 can bidirectionally transport organic cations. In light of these results, we propose that through astrocyte/neuron interactions, Oct3 may contribute to or mitigate—depending on the source of the toxic compounds—the degeneration of the ascending midbrain dopaminergic pathways. This hypothesis is particularly appealing given the growing body of literature on the role of glial cells, including astrocytes, in the demise of dopaminergic neurons in both PD and its experimental models (23).

Consistent with this proposed pathogenic scenario are our demonstrations that both the inhibition and the deletion of Oct3 in mice prevented MPTP-induced dopaminergic toxicity by blocking the release of MPP^+ (an active metabolite of MPTP) from astrocytes. These findings are significant because they provide the answer to one of the outstanding issues about MPTP toxicokinetics. As reviewed in ref. 1 and illustrated in Fig. S6, following MPTP administration, this protoxin is quickly converted into MPP^+ by MAO-B, an enzyme that is expressed primarily in astrocytes but not in dopaminergic neurons. For decades, how MPP^+ exits astrocytes without killing them has been a mystery. Our data provide compelling evidence that before entering the neighboring dopaminergic neurons, MPP^+ is released from astrocytes into the extracellular space by a plasma membrane transporter, namely Oct3. Thus, this novel piece of information is not only of critical value for our understanding of the mechanism of cell death in the widely used MPTP model of Parkinson's disease, but it may also be extended to other toxic cations. While our current knowledge is incomplete regarding the array of dopaminergic toxic cations that can be released from astrocytes through Oct3, the toxic cationic metabolites of compounds such as tetraisoquinolines and β-carbolines may be released through this mechanism on the basis of their structural similarity to MPP^+ (24, 25). For instance, tetraisoquinolines can be metabolized by MAO-B in astrocytes to form isoquinolinium cations (24) and β-carbolines can be converted to β-carbolinium in astrocytes by myeloperoxidase (26, 27). Both of these lipophillic compounds, which have been linked to Parkinson's disease, are present in the environment, in foodstuffs, and in the brain through endogenous formation (24, 28).

Conversely, under conditions where the abundance of extracellular toxic cations is normally cleared by Oct3, increased neurodegeneration may occur if Oct3 activity is reduced. This alternative paradigm is supported by our methamphetamine results. Mechanistically, regarding the nigrostriatal pathway, methamphetamine primarily destroys dopaminergic nerve terminals in the striatum, but spares dopaminergic cell bodies in substantia nigra (29). The uptake of methamphetamine into dopaminergic neurons is facilitated by DAT (30). Once inside monoaminergic neurons, methamphetamine inhibits monoamine oxidase (31), promotes flux reversal of DAT, and induces DA efflux from vesicles into the cytosol and then the extracellular compartment (32, 33). All these changes lead to a rapid increase in extracellular DA (34). It is believed that an excess of nonvesicular DA, by inducing oxidative stress through DA-related reactive products (35–37) or by microglial activation (38), is instrumental in methamphetamine-induced damage to dopaminergic structures. In our present study, however, the relationship between increased extracellular DA and neurotox-

icity does not appear to be strongly correlated. For example, although a single injection of 30 mg/kg of methamphetamine (Fig. 5*E*) produced 2- to 4-fold higher DA efflux than that produced by an injection of 5 mg/kg (Fig. 5*A*), a similar magnitude of loss in striatal TH was detected between these regimens (Fig. 5 *D* and *H*). These results suggest that extracellular DA alone cannot account for neurotoxicity. However, the observation that only a high dose of methamphetamine could induce a higher extracellular DA level in the *Oct3*$^{-/-}$ mice is consistent with a previous study in which these knockout mice exhibit much greater methamphetamine-induced locomotor activity compared to their wild-type littermates after administration of a high dose of methamphetamine (22). Together these data support the critical role of Oct3 in the removal of excess extracellular DA.

In conclusion, the present study highlights the existence of an unrecognized pathway by which Oct3 modulates neurodegeneration as seen in Parkinson's disease and methamphetamine neurotoxicity through coordinated interactions of different cell types. Polymorphisms of OCT3 have been reported in humans (39, 40). These polymorphisms may reduce or inactivate the function of OCT3 and therefore enhance the euphoria and potential for addiction (40) and susceptibility to the toxicity of substances of abuse. Strategies aimed at increasing OCT3 function may thus be beneficial in drug addiction. This is analogous to amyotrophic lateral sclerosis studies where glutamate transporter function is restored (7, 8) in astrocytes to facilitate removal of extracellular glutamate.

Methods

Animals. Wild-type C57BL/6 mice were purchased from the Charles River Laboratories. The *Slc22a3*-deficient mice were kindly shared with us by B. Giros and S. Gautron (Inserm, Creteil, France). These mutant mice were generated by homologous recombination as described previously (41). The expression of Oct3 is completely abolished in all tissues, including the brain, of adult homozygous mutant mice (41). These animals were backcrossed with C57BL/6 mice for 6 generations to generate heterozygous breeders. All experiments were approved by the Institution Animal Care and Use Committee of the University of Rochester.

See *SI Materials and Methods* for MPTP and methamphetamine treatments, human samples, immunohistochemistry, real time qRT-PCR, stereological cell count, LCM, in vivo microdialysis, HPLC measurements of striatal DA and MPP$^+$ levels, cell cultures, and transport assays.

Statistics. All values are expressed as mean ± SEM. Differences between means were analyzed using either 1-way or 2-way ANOVA followed by Newman-Keuls post hoc testing for pairwise comparison using SigmaStat v3.5. For in vivo microdialysis data, areas under the curve were generated using GraphPad Prism v5.01 followed by a 2-tailed *t* test. The null hypothesis was rejected when *P*-value was <0.05.

ACKNOWLEDGMENTS. We are grateful to Dr. Maiken Nedergaard for critically reading this manuscript and for the confocal microscope, to Dr. Berislav Zlokovic for the LCM equipment, and to Robert Bell for assisting in setting up this technique. We thank Drs. Bruno Giros and Sophie Gautron for the *Oct3*$^{-/-}$ breeders. We thank Meghan Blair for her assistance in maintaining these mouse colonies and for methamphetamine injections, Dr. Namita Sen for assessing D22 on DAT function, Dr. Weiguo Peng for assisting in setting up in vivo microdialysis, and Dr. Paula Ashe for assisting in preparing this manuscript. This study is supported in part by National Institutes of Health Grants ES014899, P30 ES01247, and T32 ES07026. J.P. is also the recipient of a National Institute of Environmental Health Sciences Undergraduate Award (ES014899–02S1). S.P. is supported by National Institutes of Health Grants NS0641912, NS062180, NS042269, NS38370-09, and AG021617; the U.S. Department of Defense Awards W81WXWH-08-1-0465 and W81WXWH-08-1-0522; the Parkinson's Disease Foundation; The Thomas Hartman Foundation for Parkinson's Research; and he is the recipient of the Page and William Black Chair of Neurology.

1. Dauer W, Przedborski S (2003) Parkinson's disease: Mechanisms and models. *Neuron* 39:889–909.
2. Miller GW, Gainetdinov RR, Levey AI, Caron MG (1999) Dopamine transporters and neuronal injury. *Trends Pharmacol Sci* 20:424–429.
3. Nagai M, et al. (2007) Astrocytes expressing ALS-linked mutated SOD1 release factors selectively toxic to motor neurons. *Nat Neurosci* 10:615–622.
4. Custer SK, et al. (2006) Bergmann glia expression of polyglutamine-expanded ataxin-7 produces neurodegeneration by impairing glutamate transport. *Nat Neurosci* 9:1302–1311.
5. Shin JY, et al. (2005) Expression of mutant huntingtin in glial cells contributes to neuronal excitotoxicity. *J Cell Biol* 171:1001–1012.
6. Das S, Potter H (1995) Expression of the Alzheimer amyloid-promoting factor antichymotrypsin is induced in human astrocytes by IL-1. *Neuron* 14:447–456.
7. Guo H, et al. (2003) Increased expression of the glial glutamate transporter EAAT2 modulates excitotoxicity and delays the onset but not the outcome of ALS in mice. *Hum Mol Genet* 12:2519–2532.
8. Lepore AC, et al. (2008) Focal transplantation-based astrocyte replacement is neuroprotective in a model of motor neuron disease. *Nat Neurosci* 11:1294–1301.
9. Javitch JA, D'Amato RJ, Strittmatter SM, Snyder SH (1985) Parkinsonism-inducing neurotoxin, N-methyl-4-phenyl-1,2,3,6-tetrahydropyridine: Uptake of the metabolite N-methyl-4-phenylpyridinium by dopamine neurons explain selective toxicity. *Proc Natl Acad Sci USA* 82:2173–2177.
10. Grundemann D, Schechinger B, Rappold GA, Schomig E (1998) Molecular identification of the corticosterone-sensitive extraneuronal catecholamine transporter. *Nat Neurosci* 1:349–351.
11. Amphoux A, et al. (2006) Differential pharmacological in vitro properties of organic cation transporters and regional distribution in rat brain. *Neuropharmacology* 50:941–952.
12. Kekuda R, et al. (1998) Cloning and functional characterization of a potential-sensitive, polyspecific organic cation transporter (OCT3) most abundantly expressed in placenta. *J Biol Chem* 273:15971–15979.
13. Wu X, et al. (1998) Identity of the organic cation transporter OCT3 as the extraneuronal monoamine transporter (uptake2) and evidence for the expression of the transporter in the brain. *J Biol Chem* 273:32776–32786.
14. Vialou V, et al. (2004) Organic cation transporter 3 (Slc22a3) is implicated in salt-intake regulation. *J Neurosci* 24:2846–2851.
15. Giovanni A, Sieber BA, Heikkila RE, Sonsalla PK (1991) Correlation between the neostriatal content of the 1-methyl-4- phenylpyridinium species and dopaminergic neurotoxicity following 1-methyl-4-phenyl-1,2,3,6-tetrahydropyridine administration to several strains of mice. *J Pharmacol Exp Ther* 257:691–697.
16. Russ H, et al. (1993) Cyanine-related compounds: A novel class of potent inhibitors of extraneuronal noradrenaline transport. *Naunyn Schmiedebergs Arch Pharmacol* 348:458–465.
17. Rollema H, et al. (1988) MPP+-induced efflux of dopamine and lactate from rat striatum have similar time courses as shown by in vivo brain dialysis. *J Pharmacol Exp Ther* 245:858–866.
18. Dauer W, et al. (2002) Resistance of alpha-synuclein null mice to the parkinsonian neurotoxin MPTP. *Proc Natl Acad Sci USA* 99:14524–14529.
19. Santiago M, Machado A, Cano J (2001) Validity of a quantitative technique to study striatal dopaminergic neurodegeneration by in vivo microdialysis. *J Neurosci Methods* 108:181–187.
20. Matsubara K, et al. (1996) Differences in dopamine efflux induced by MPP+ and beta-carbolinium in the striatum of conscious rats. *Eur J Pharmacol* 315:145–151.
21. Gasser PJ, Orchinik M, Raju I, Lowry CA (2009) Distribution of organic cation transporter 3, a corticosterone-sensitive monoamine transporter, in the rat brain. *J Comp Neurol* 512:529–555.
22. Vialou V, et al. (2008) Altered aminergic neurotransmission in the brain of organic cation transporter 3-deficient mice. *J Neurochem* 106:1471–1482.
23. Przedborski S (2007) Neuroinflammation and Parkinson's disease. *Handb Clin Neurol* 83:535–551.
24. McNaught KS, et al. (1998) Isoquinoline derivatives as endogenous neurotoxins in the aetiology of Parkinson's disease. *Biochem Pharmacol* 56:921–933.
25. Albores R, et al. (1990) Mitochondrial respiratory inhibition by N-methylated beta-carboline derivatives structurally resembling N-methyl-4-phenylpyridine. *Proc Natl Acad Sci USA* 87:9368–9372.
26. Herraiz T, Guillen H, Galisteo J (2007) N-methyltetrahydro-beta-carboline analogs of 1-methyl-4-phenyl-1,2,3,6-tetrahydropyridine (MPTP) neurotoxin are oxidized to neurotoxic beta-carbolinium cations by heme peroxidases. *Biochem Biophys Res Commun* 356:118–123.
27. Choi DK, et al. (2005) Ablation of the inflammatory enzyme myeloperoxidase mitigates features of Parkinson's disease in mice. *J Neurosci* 25:6594–6600.
28. Neafsey EJ, et al. (1995) Methyl-beta-carbolinium analogs of MPP+ cause nigrostriatal toxicity after substantia nigra injections in rats. *Brain Res* 675:279–288.
29. Axt KJ, Mamounas LA, Molliver ME (1994) in *Amphetamine and Its Analogs. Psychopharmacology, Toxicology, and Abuse*, eds Cho AK and Segal DS (Academic, New York), pp 315–367.
30. Fumagalli F, Gainetdinov RR, Valenzano KJ, Caron MG (1998) Role of dopamine transporter in methamphetamine-induced neurotoxicity: Evidence from mice lacking the transporter. *J Neurosci* 18:4861–4869.
31. Scorza MC, et al. (1997) Monoamine oxidase inhibitory properties of some methoxylated and alkylthio amphetamine derivatives: Structure-activity relationships. *Biochem Pharmacol* 54:1361–1369.
32. Sulzer D, et al. (1995) Amphetamine redistributes dopamine from synaptic vesicles to the cytosol and promotes reverse transport. *J Neurosci* 15:4102–4108.
33. Kita T, et al. (2000) Methamphetamine-induced striatal dopamine release, behavior changes and neurotoxicity in BALB/c mice. *Int J Dev Neurosci* 18:521–530.
34. Clausing P, Bowyer JF (1999) Time course of brain temperature and caudate/putamen microdialysate levels of amphetamine and dopamine in rats after multiple doses of d-amphetamine. *Ann N Y Acad Sci* 890:495–504.
35. Cubells JF, Rayport S, Rajendran G, Sulzer D (1994) Methamphetamine neurotoxicity involves vacuolation of endocytic organelles and dopamine-dependent intracellular oxidative stress. *J Neurosci* 14:2260–2271.
36. Fumagalli F, et al. (1999) Increased methamphetamine neurotoxicity in heterozygous vesicular monoamine transporter 2 knock-out mice. *J Neurosci* 19:2424–2431.
37. Cadet JL, Krasnova IN, Jayanthi S, Lyles J (2007) Neurotoxicity of substituted amphetamines: Molecular and cellular mechanisms. *Neurotox Res* 11:183–202.
38. Thomas DM, Francescutti-Verbeem DM, Kuhn DM (2008) The newly synthesized pool of dopamine determines the severity of methamphetamine-induced neurotoxicity. *J Neurochem* 105:605–616.
39. Lazar A, et al. (2003) Genetic variability of the extraneuronal monoamine transporter EMT (SLC22A3). *J Hum Genet* 48:226–230.
40. Aoyama N, et al. (2006) Association between gene polymorphisms of SLC22A3 and methamphetamine use disorder. *Alcohol Clin Exp Res* 30:1644–1649.
41. Zwart R, et al. (2001) Impaired activity of the extraneuronal monoamine transporter system known as uptake-2 in Orct3/Slc22a3-deficient mice. *Mol Cell Biol* 21:4188–4196.
42. Callahan BT, et al. (2001) Inhibitors of Na(+)/H(+) and Na(+)/Ca(2+) exchange potentiate methamphetamine-induced dopamine neurotoxicity: Possible role of ionic dysregulation in methamphetamine neurotoxicity. *J Neurochem* 77:1348–1362.